# Odd discrete Fourier transforms for the analysis of Schwarz domain decomposition methods discretized with finite volume schemes

Laurence Halpern[0000−0002−7877−7130] and
Martin Gander[0000−0001−8450−9223] and
Florence Hubert[0000−0002−7553−9698] and
Stella Krell[0009−0006−2206−0882]

## 1 Odd Fourier series for studying Schwarz methods

The analysis and optimization of Schwarz methods is well understood for Laplace type problems on unbounded domains, and the main tool is Fourier transforms. We present here a new approach for studying and optimizing Schwarz methods in bounded geometries, applied to anisotropic diffusion, and also in a fully discrete setting when using finite volume discretizations. To this end, we extend the Fourier analysis to odd Fourier transforms, and combine it with asymptotic techniques relying on known equioscillation results for simpler cases. We show that this allows us to gain the main highly accurate insight and optimization results of Schwarz methods.

Let $u \in H^1(0,Y)$ with boundary values $u(0) = u(Y) = 0$. We extend $u$ classically to $\tilde{u}$, a periodic function on $\mathbb{R}$, first by an odd extension for $y \in (0,Y)$, *i.e.* $\tilde{u}(y) = u(y)$ and $\tilde{u}(y) = -u(-y)$ for $y \in (-Y,0)$, and then by periodicity with period $2Y$, *i.e.* $\tilde{u}(y+2mY) = \tilde{u}(y)$ for $y \in (-Y,Y)$ and $m \in \mathbb{Z}$. The odd Fourier series of $u$ is then defined as the Fourier series of $\tilde{u}$, $\tilde{u}(y) = \sum_{k\in\mathbb{Z}} \hat{u}(k) e^{i\omega k y}$ with $\omega = \frac{\pi}{Y}$, and $\hat{u}(k) = \int_{-Y}^{Y} \tilde{u}(y) e^{-i\omega k y} \frac{dy}{2Y}$.

The odd Fourier series is an essential analysis tool for studying and optimizing Schwarz methods in rectangular geometry applied to anisotropic diffusion,

$$\eta u - A_{xx}\partial_{xx}u - 2A_{xy}\partial_{xy}u - A_{yy}\partial_{yy}u = f, \quad \Omega = (-X_1, X_2) \times (0,Y), \qquad (1)$$

Martin J. Gander
Section de Mathématiques, Université de Genève, Switzerland, e-mail: martin.gander@unige.ch

Laurence Halpern
LAGA, Université Sorbonne Paris-Nord, France, e-mail: halpern@math.univ-paris13.fr

Florence Hubert
Aix-Marseille Université, CNRS, I2M, Marseille, FRANCE, e-mail: florence.hubert@univ-amu.fr

Stella Krell
Université Côte d'Azur, Inria, CNRS, LJAD, France, e-mail: stella.krell@univ-cotedazur.fr

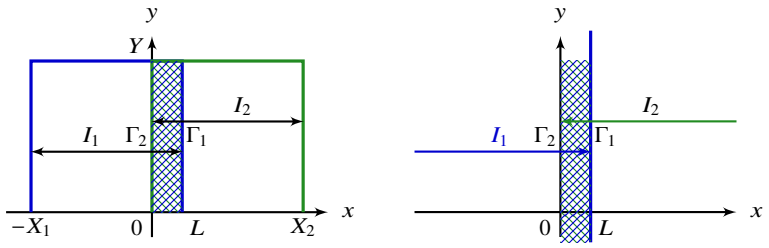


**Fig. 1** Domain decomposition in the $x$ direction for anisotropic diffusion. Left: new situation considered here with rectangular subdomains $\Omega_1 = (-X_1, L) \times (0, Y)$ and $\Omega_2 = (0, X_2) \times (0, Y)$. Right: half-plane subdomains $\Omega_1 = (-\infty, L) \times \mathbb{R}$ and $\Omega_2 = (0, \infty) \times \mathbb{R}$, well understood using Fourier transforms.

with homogeneous Dirichlet boundary conditions. Consider two subdomains, as shown in Figure 1 on the left. The iterates $u_j^\ell$ of an alternating Schwarz method with Ventcell transmission conditions are defined by equation (1) in the subdomains, and the transmission conditions

$$\begin{aligned}(\partial_{\nu_A} + p - qA_{yy}\partial_{yy})u_1^\ell(L, y) &= (\partial_{\nu_A} + p - qA_{yy}\partial_{yy})u_2^{\ell-1}(L, y),\\ (-\partial_{\nu_A} + p - qA_{yy}\partial_{yy})u_2^\ell(0, y) &= (-\partial_{\nu_A} + p - qA_{yy}\partial_{yy})u_1^\ell(0, y),\end{aligned} \tag{2}$$

where $\partial_{\nu_A} = A_{xx}\partial_x + A_{xy}\partial_y$ is the normal derivative in the metric defined by $A$. The coefficients $p$ and $q$ are positive, and $q = 0$ corresponds to Robin operators. Note that the transmission operators include the classical Dirichlet case by letting $p$ tend to infinity. The algorithm is well defined when starting with an initial guess $g(y)$ applied at iteration step $\ell = 1$ in $\Omega_1$, $(\partial_{\nu_A} + p - qA_{yy}\partial_{yy})u_1^1(L, y) = g(y)$. We denote the odd and periodic extensions of $f$, $g$, $u$ and $u_j^\ell$ in the variable $y$ with a tilde. Then the equations (1) and (2) are satisfied for the tilde functions in $\tilde{\Omega} = (-X_1, X_2) \times \mathbb{R}$. The error at step $\ell$, $(\tilde{e}_1^\ell, \tilde{e}_2^\ell)$, is solution of the homogeneous equation ($f = 0$), with the same transmission conditions. We apply the odd Fourier series in $y$ to equation (1) with $f = 0$, with $\hat{e}_j^\ell(x, k)$ the odd Fourier series error coefficients which satisfy

$$-A_{xx}\partial_{xx}\hat{e}_j^\ell - 2i\omega k A_{xy}\partial_x\hat{e}_j^\ell + (\eta + (\omega k)^2 A_{yy})\hat{e}_j^\ell = 0. \tag{3}$$

The characteristic polynomial for (3) has two roots,

$$r_\pm(k) = \frac{-i\omega k A_{xy} \pm D(\omega k)}{A_{xx}}, \quad D(\xi) = \sqrt{\eta A_{xx} + \xi^2 \det A} > 0. \tag{4}$$

With the notation $\tilde{D}(\xi) = \frac{D(\xi)}{A_{xx}}$, the solutions in the subdomains are

$$\hat{e}_1(x, k) = \alpha_1(k) e^{\frac{-i\omega k A_{xy}}{A_{xx}}(x + X_1)} \sinh(\tilde{D}(\omega k)(x + X_1)), \tag{5}$$

$$\hat{e}_2(x, k) = \alpha_2(k) e^{\frac{-i\omega k A_{xy}}{A_{xx}}(x - X_2)} \sinh(\tilde{D}(\omega k)(x - X_2)). \tag{6}$$

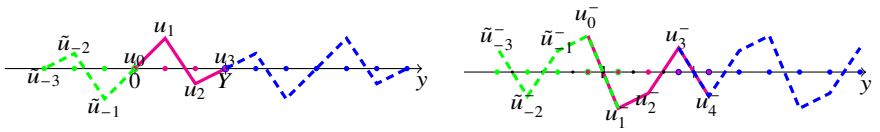


Vertex centered scheme.
$u_0 = u_N = 0$.

Cell centered scheme.
$u^-_0 + u^-_1 = 0, \quad u^-_N + u^-_{N+1} = 0$.

**Fig. 2** The odd and periodic extension for the vertex and cell centered schemes. $Nh_y = Y$, $N = 3$.

The convergence factor $\rho$ is obtained by successive application of the transmission conditions (2), and with $S(\xi) = p + qA_{yy}\xi^2$ , we obtain after a short computation

$$\rho(k, L, X_1, X_2) = \frac{S(\omega k)\sinh(\tilde{D}(\omega k)(X_2 - L)) - D(\omega k)\cosh(\tilde{D}(\omega k)(X_2 - L))}{S(\omega k)\sinh(\tilde{D}(\omega k)X_2) + D(\omega k)\cosh(\tilde{D}(\omega k)X_2)} \times \frac{S(\omega k)\sinh(\tilde{D}(\omega k)X_1) - D(\omega k)\cosh(\tilde{D}(\omega k)X_1)}{S(\omega k)\sinh(\tilde{D}(\omega k)(X_1 + L)) + D(\omega k)\cosh(\tilde{D}(\omega k)(X_1 + L))}. \quad (7)$$

In the infinite case in Figure 1 (right), $X_1 = X_2 = +\infty$, the convergence factor simplifies to

$$\rho_\infty(k, L) = \left(\frac{S(\omega k) - D(\omega k)}{S(\omega k) + D(\omega k)}\right)^2 e^{-2LD(\omega k)/A_{xx}}, \quad (8)$$

where the exponential term is the convergence factor for Dirichlet transmission conditions , *i.e.* as $p$ tends to infinity. It is clearly smaller than 1, and it is also smaller for Ventcell transmission conditions than for Dirichlet transmission conditions. The analysis for the rectangular case is the same as in the discrete case of Theorem 2 below.

## 2 Discretization and the odd discrete Fourier transform

We consider both vertex and cell centered finite volume discretizations. They differ not only by the location where the values are taken (node $y_j$ for vertex-centered, and $y^-_j = y_j - \frac{h_y}{2}$ for cell-centered, see Figure 2), but as a consequence also by the way boundary conditions are imposed. The extension $\tilde{\mathbf{u}}$ of the vector $\mathbf{u} = (u_0, \ldots, u_N)$ in the vertex-centered case or $\mathbf{u} = (u^-_0, \ldots, u^-_{N+1})$ in the cell-centered case (in magenta in Figure 2), is obtained by odd extension (in green) and periodisation with period $2N$ (in blue). More precisely the piecewise affine function linking the nodes is odd and periodic.

The odd discrete Fourier transform of the vector $\mathbf{u}$ is defined using the classical discrete Fourier transform of $\tilde{\mathbf{u}}$: for $-(N-1) \le k \le N$, we have in the vertex-

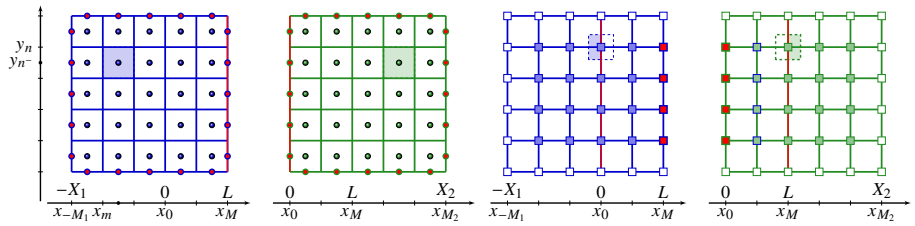


**Fig. 3** FV4 schemes in 2D: Cell-centered (left), Vertex -centered (right). Overlap $L$

centered (vc) case $\hat{u}(k) = \sum_{n=-(N-1)}^{N} \tilde{u}_n \, e^{-i\pi k \frac{n}{N}}$ , and in the cell-centered (cc) case $\hat{u}(k) = \sum_{n=-(N-1)}^{N} \tilde{u}_n^- \, e^{-i\pi k \frac{n}{N}}$.

We use finite volumes in both directions, $x$ and $y$, for the discretization of Problem (1), see Figure 3 for an illustration. Assuming that $A_{xy} = 0$ in the anisotropic diffusion equation (1), the discrete equation for the error (with $f = 0$) is

$$-A_{xx} D_x^+ D_x^- \mathbf{u} - A_{yy} D_y^+ D_y^- \mathbf{u} + \eta \mathbf{u} = 0,$$

were $D^+$ and $D^-$ are the classical forward and backward finite difference operators, e.g. $D_x^+ u(m,n) = \frac{1}{h_x}(u(m+1,n) - u(m,n))$. We extend the equation to $n \in \mathbb{Z}$, with solution $\tilde{\mathbf{u}}$, and Fourier transform it in the discrete $y$ direction to

$$(\eta + \frac{4A_{yy} \sin^2(\frac{\pi k}{2N})}{h_y^2})\hat{u}(m,k) - \frac{A_{xx}}{h_x^2}(\hat{u}(m+1,k) - 2\hat{u}(m,k) + \hat{u}(m-1,k)) = 0,$$

where $m$ stands for the discrete index in the $x$ direction, and $k$ for the discrete Fourier index in the $y$ direction. This is a difference equation which can be solved in the subdomains. Let $\mathbf{u}_j^\ell$ be the discrete iterate in domain $\Omega_j$, and $\mathbf{e}_j^\ell = \mathbf{u} - \mathbf{u}_j^\ell$ be the discrete error. Suppose that $X_1 = M_1 h_x$, $X_2 = M_2 h_x$, and $L = M h_x$. With the definitions

$$\beta(k) = \frac{2}{h_y} \sin(\frac{\pi k}{2N}), \; \mu(k) = \frac{h_x^2}{A_{xx}}(A_{yy}\beta^2(k) + \eta), \quad 2\sinh(\nu/2) = \sqrt{\mu}, \tag{9}$$

we find after a short calculation the errors in the subdomains for the vertex centered scheme to be

$$\hat{\mathbf{e}}_1^\ell(m,k) = b_1^\ell(k) \sinh(\nu(k)(M_1 + m)), \; \hat{\mathbf{e}}_2^\ell(m,k) = b_2^\ell(k) \sinh(\nu(k)(M_2 - m)), \tag{10}$$

and similarly for the cell-centered scheme, with $m^-$ replacing $m$. The discretization of the transmission conditions is achieved with the discrete operator $A_{xx} D_x^\pm + p - q A_{yy} D_y^+ D_y^-$. We then obtain after a short computation as in the continuous case the convergence factor for the vertex centered scheme in bounded domains with Ventcell transmission conditions to be

$$\rho_{vc}(k,M,M_1,M_2) = \frac{S(\beta)\sinh(\nu(M_2-M)) - \frac{A_{xx}}{h_x}\sinh\nu\cosh(\nu(M_2-M))}{S(\beta)\sinh(\nu M_2) + \frac{A_{xx}}{h_x}\sinh\nu\cosh(\nu M_2)} \times \frac{S(\beta)\sinh(\nu M_1) - \frac{A_{xx}}{h_x}\sinh\nu\cosh(\nu M_1)}{S(\beta)\sinh(\nu(M_1+M)) + \frac{A_{xx}}{h_x}\sinh\nu\cosh(\nu(M_1+M))}, \quad (11)$$

where $\beta = \beta(k)$ and $\nu = \nu(\beta(k))$.

It is similar to the continuous convergence factor in (7), with $\tilde{D}(\omega k)$ replaced by $\nu(k)/h_x$. The convergence factor of the cell-centered scheme is obtained by simply exchanging $\sinh\nu$ with $2\tanh\frac{\nu}{2}$ in (11). In the infinite case of Figure 1 (right), $M_1 = M_2 = +\infty$, the convergence factors simplify to

$$\begin{aligned} \rho_{vc,\infty}(k,M) &= \left(\frac{S(\beta) - \frac{A_{xx}}{h_x}\sinh\nu}{S(\beta) + \frac{A_{xx}}{h_x}\sinh\nu}\right)^2 e^{-2M\nu}, \\ \rho_{cc,\infty}(k,M) &= \left(\frac{S(\beta) - 2\frac{A_{xx}}{h_x}\tanh\left(\frac{\nu}{2}\right)}{S(\beta) + 2\frac{A_{xx}}{h_x}\tanh\left(\frac{\nu}{2}\right)}\right)^2 e^{-2M\nu}. \end{aligned} \quad (12)$$

**Theorem 1 (Infinite subdomains, Figure 1 (right))** *In the case of infinite subdomains, $M_1, M_2 \to \infty$, the Schwarz algorithm discretized with a vertex or cell centered scheme, with Dirichlet transmission conditions and overlap $M > 0$ is convergent. When Ventcell transmission conditions are used with $p > 0$ and $q \geq 0$, it is convergent with and without overlap. With overlap it converges faster with Ventcell transmission conditions than with Dirichlet transmission conditions.*

*Proof.* In the Dirichlet case, the convergence factor for both discretizations is the same, we call it $\rho^D_{d,\infty} = e^{-2\nu M} < 1$. Furthermore the factors in front of $\rho^D_{d,\infty}$ in (12) are also smaller than 1, and hence the result follows. □

**Theorem 2 (Bounded subdomains, Figure 1 (left))** *In the case of bounded subdomains, the Schwarz algorithm discretized with a vertex centered or cell-centered scheme, with Dirichlet transmission conditions with overlap $M > 0$ is convergent. When Ventcell transmission conditions are used with $p > 0$ and $q \geq 0$, it is convergent with or without overlap. If $M \geq 1$, there exists a $p_0$ depending on the coefficients of the problem such that if $p > p_0$, the algorithm converges faster with Ventcell transmission conditions than with Dirichlet transmission conditions i.e. for any $k$ with $-(N-1) \leq k \leq N$, $|\rho_d(k,M,M_1,M_2)| < |\rho^D_d(k,M,M_1,M_2)|$, for $d = cc$ or $vc$.*

*Proof.* In the Dirichlet case, the convergence factor for both discretizations is the same, depending on $\nu$ directly, namely

$$\rho^D_d(k,M,M_1,M_2) = \frac{\sinh(M_1\nu)}{\sinh((M_1+M)\nu)}\,\frac{\sinh((M_2-M)\nu)}{\sinh(M_2\nu)}, \quad (13)$$

and each factor is smaller than 1 since the function sinh is increasing. For the Ventcell condition in the vertex centered case, we need a lemma:

**Lemma 1** *For any real numbers $0 < x < y$, and any positive real numbers a and b,*

$$-1 < \frac{a\sinh x - b\cosh x}{a\sinh y + b\cosh y} < 1. \tag{14}$$

*Proof.* The proof is obtained by multiplying with the denominator on both sides, and using the monotonicity properties of sinh and cosh. □

We now apply Lemma 1 successively to each factor in (11) with $(x, y) = (M_2 - M, M_2)$ for the first one, and $(x, y) = (M_1, M_1 + M)$ for the second one to conclude that the convergence factor in modulus is smaller than 1.

To compare the Ventcell and Dirichlet case, setting $\alpha = A_{yy}\beta^2$, we factor out the convergence factor for Dirichlet as

$$\begin{aligned}\rho_{vc}(k, M, M_1, M_2) \;=\; & \frac{(p + q\alpha) - \dfrac{A_{xx}}{h_x}\sinh\nu\coth(\nu M_1)}{(p + q\alpha) + \dfrac{A_{xx}}{h_x}\sinh\nu\coth(\nu(M_1 + M))} \\ & \times \frac{(p + q\alpha) - \dfrac{A_{xx}}{h_x}\sinh\nu\coth(\nu(M_2 - M))}{(p + q\alpha) + \dfrac{A_{xx}}{h_x}\sinh\nu\coth(\nu M_2)}\rho^D_{vc}(k, M, M_1, M_2).\end{aligned} \tag{15}$$

The first two factors on the right are clearly smaller than 1. They are both greater that -1 if and only if

$$\begin{aligned}2(p + q\alpha) &> \frac{A_{xx}}{h_x}\sinh\nu(\coth(\nu M_1) - \coth(\nu(M_1 + M))), \\ 2(p + q\alpha) &> \frac{A_{xx}}{h_x}\sinh\nu(\coth(\nu(M_2 - M)) - \coth(\nu M_2))).\end{aligned} \tag{16}$$

Consider the function $\Phi_1(\nu) = \sinh\nu(\coth(\nu M_1) - \coth(\nu(M_1 + M)))$. Since coth is decreasing from $+\infty$ to 1, $\Phi_1$ is a positive function, and by a first order Taylor expansion of $\sinh x \sim x$ as $x \to 0$, we have

$$\lim_{\nu\to 0}\Phi_1(\nu) = \frac{1}{M_1} - \frac{1}{M_1 + M} > 0.$$

To expand at infinity, we use that $\coth x \sim 1 + 2e^{-2x}$ at infinity to see that, as $\nu$ tends to infinity,

$$\Phi_1(\nu) \sim e^{\nu}(e^{-\nu M_1} - e^{-\nu(M_1+M)}) \sim e^{\nu(1-M_1)} \to 0.$$

The function $\Phi_1$ is therefore bounded on $\mathbb{R}_+$, and similarly also the function $\Phi_2(\nu) = \sinh\nu(\coth(\nu(M_2 - M)) - \coth(\nu M_2)))$. So if $p$ is larger than the corresponding two maxima in the inequalities (16), they hold and for any $\alpha$, that is any frequency, $|\rho_{vc}(k, M, M_1, M_2)| < |\rho^D_{vc}(k, M, M_1, M_2)|$. For the discrete cell centered case, the calculations are analogous, using the properties of the hyperbolic tangent. □

## 3 Value for Domain Decomposition Analysis

The convergence factor in bounded domains (11) announced in [3] contains all simplified situations from [5, 4]: the classical Dirichlet case is obtained by letting $p$ tend to infinity in (11); the nonoverlapping case is obtained by letting $M$ go to 0; the unbounded case is obtained by letting $M_1$ and $M_2$ tend to infinity as in (8, 12). Existence results for the optimized parameters on the interval $(1, N)$ in the continuous case when $X_1 = X_2$ (subdomains of equal size) and $M = 0$ (no overlap) can be found in [4], where also exact formulas in the Robin case, and a set of algebraic equations in the Ventcell case can be found. These results were obtained by homographic best approximation introduced in [1], characterized by equioscillation properties. Equioscillation also allows one to obtain asymptotic formulas which can be a useful and efficient replacement for implicit equations. The best approximation results also hold in the discrete case, building on general results in [5].

However, when the subdomains are not of equal size, $X_1 \neq X_2$, or there is overlap, $M \neq 0$, proving existence results seems to be a difficult task and is currently out of reach. There are two alternative strategies: the first one is to compute optimized parameters using numerical optimization for specific values of the parameters arising in a domain decomposition simulation. The second is to use asymptotic analysis in order to obtain closed form formulas for the optimized parameters which are valid when the mesh size (or other parameters) become small (or large). Such asymptotic parameters can be very useful, and also give more insight (for applications to nonlinear problems for instance, see [2]).

As an example, we show now in detail how one can asymptotically optimize parameters for the continuous convergence factor for Ventcel l transmission conditions ($p > 0$, $q > 0$) without overlap, $L = 0$. In the case $X_1 = X_2$, it was proved in [4] that $\rho$ in (7) has an extremum point $\bar{k} \in (1, N)$, *i.e.* $\partial_k \rho(\bar{k}) = 0$. The coefficients $(p, q)$ are then characterized, by the Theorem of de la Vallée Poussin, by the condition that the values of $\rho$ at $(1, \bar{k}, N)$ equioscillate. This gives 3 equations for the 3 unknowns $p$, $q$ and $\bar{k}$, which can be solved asymptotically for large $N$. Based on this insight, we can obtain asymptotically optimized parameters for the general case $X_1 \neq X_2$ as follows: we assume as for the case $X_1 = X_2$ the asymptotic behavior

$$\text{(i) } p = C_p N^{1/4}, \quad \text{(ii) } q = C_q N^{-3/4}, \quad \text{(iii) } \bar{k} = C N^{1/2}, \tag{17}$$

and study $\rho$ in (7) asymptotically for $k$ large. For $k$ large, the hyperbolic sine and cosine terms are equivalent, and the fact that we know the asymptotic behavior from (17) simplifies the asymptotic expansion computations considerably. We find

$$\begin{aligned} &\rho(1) \sim 1 - \tfrac{4}{C_p} D_{12} N^{-1/4}, \quad \rho(N) \sim 1 - 4 \tfrac{\sqrt{\det A}}{C_q A_{yy}} N^{-1/4}, \\ &\partial_k \rho(\bar{k}) = 0 \implies A_{yy} C_{\bar{k}}^2 C_q - C_p = 0, \quad \rho(\bar{k}) \sim 1 - 4 \tfrac{2C_p}{\sqrt{det A C}} N^{-1/4}, \end{aligned} \tag{18}$$

with $\det A = A_{xx} A_{yy} - A_{xy}^2$, and $D_{12} = D(\omega)(\coth(X_1 \tilde{D}(\omega)) + \coth(X_2 \tilde{D}(\omega))$. Equating asymptotically the values of $\rho$ at the three points gives closed form asymp-

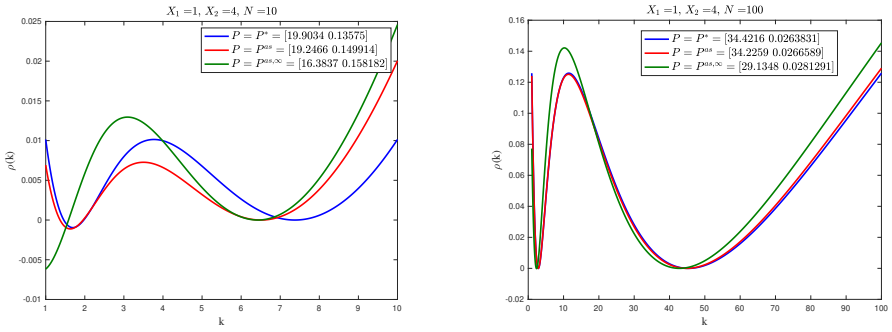


**Fig. 4** Convergence factors $\rho$ for $X_1 = 1$, $X_2 = 4$, $Y = 1$. Left: $N = 10$. Right: $N = 100$. $P = [p, q]$.

totic formulas for the best parameters and best convergence factor,

$$p^{as}(0, X_1, X_2) \sim \frac{\det A^{1/8} D_{12}^{3/4}}{\sqrt{2}} N^{1/4}, \quad q^{as}(0, X_1, X_2) \sim \frac{\det A^{5/8} D_{12}^{-1/4}}{A_{yy}\sqrt{2}} N^{-3/4},$$
$$\rho^{as}(0, X_1, X_2) \sim \rho(1, 0, X_1, X_2) \sim 1 - 4\sqrt{2} D_{12}^{1/4} \det A^{-1/8} N^{-1/4}.$$

We show as an example the results for diagonal diffusion $A_{xx} = 16$, $A_{yy} = 1$, $A_{xy} = 0$ and Ventcell transmission conditions at the continuous level without overlap in Figure 4. The blue curve represents the convergence factor with a numerical optimization to find the best parameters, the red curve uses the asymptotic parameters for bounded domains, and the green line uses the optimized parameters for the infinite domain. We see how close the asymptotic parameters are to the best parameters, and how important the bounded analysis is. The complete analysis and results for all continuous and discrete cases will appear in [6].

## References

1. Bennequin, D., Gander, M.J., Halpern, L.: A homographic best approximation problem with application to optimized Schwarz waveform relaxation. Math. Comp. **78**(265), 185–223 (2009)
2. Caetano, F., Gander, M.J., Halpern, L., Szeftel, J.: Schwarz waveform relaxation algorithms for semilinear reaction-diffusion equations. Netw. Heterog. Media **5**(3), 487–505 (2010)
3. Gander, M.J., Halpern, L., Hubert, F., Krell, S.: Optimized overlapping DDFV Schwarz algorithm. In: Finite Volumes for Complex Applications IX,, *Proceedings in Mathematics and Statistics.*, vol. 323, p. 365–373. Springer (2020)
4. Gander, M.J., Halpern, L., Hubert, F., Krell, S.: Optimized Schwarz methods with general Ventcell transmission conditions for fully anisotropic diffusion with discrete duality finite volume discretizations. Moroccan Journal of Pure and Applied Analysis **7**, 182–213 (2020)
5. Gander, M.J., Halpern, L., Hubert, F., Krell, S.: Discrete optimization of Robin transmission conditions for anisotropic diffusion with discrete duality finite volume methods. Vietnam Journal of Mathematics **49**, 1349–1378 (2021)
6. Gander, M.J., Halpern, L., Hubert, F., Krell, S.: An asymptotic procedure for optimized Schwarz methods in a discrete setting. In preparation (2026)